15 Terazaki Y, Yano S, Yuge K, Nagano S, Fukunaga M, Guo ZS *et al.* An optimal therapeutic expression level is crucial for suicide gene therapy for hepatic metastatic cancer in mice. *Hepatology* 2003; **37**: 155–163.
16 Yeung F, Law WK, Yeh CH, Westendorf JJ, Zhang Y, Wang R *et al.* Regulation of human osteocalcin promoter in hormone-independent human prostate cancer cells. *J Biol Chem* 2002; **277**: 2468–2476.
17 Sneddon WB, Demay MB. Characterization of an enhancer required for 1,25-dihydroxyvitamin D3-dependent transactivation of the rat osteocalcin gene. *J Cell Biochem* 1999; **73**: 400–407.
18 Fanburg-Smith JC, Bratthauer GL, Miettinen M. Osteocalcin and osteonectin immunoreactivity in extraskeletal osteosarcoma: a study of 28 cases. *Hum Pathol* 1999; **30**: 32–38.
19 Yuge K, Takahashi T, Nagano S, Terazaki Y, Murofushi Y, Ushikoshi H *et al.* Adenoviral gene transduction of hepatocyte growth factor elicits inhibitory effects for hepatoma. *Int J Oncol* 2005; **27**: 77–85.
20 Nagano S, Yuge K, Fukunaga M, Terazaki Y, Fujiwara H, Komiya S *et al.* Gene therapy eradicating distant disseminated micro-metastases by optimal cytokine expression in the primary lesion only: novel concepts for successful cytokine gene therapy. *Int J Oncol* 2004; **24**: 549–558.
21 Kawai T, Takahashi T, Esaki M, Ushikoshi H, Nagano S, Fujiwara H *et al.* Efficient cardiomyogenic differentiation of embryonic stem cell by fibroblast growth factor 2 and bone morphogenetic protein 2. *Circ J* 2004; **68**: 691–702.
22 Ushikoshi H, Takahashi T, Chen X, Khai NC, Esaki M, Goto K *et al.* Local overexpression of HB-EGF exacerbates remodeling following myocardial infarction by activating noncardiomyocytes. *Lab Invest* 2005; **85**: 862–873.
23 Mizuguchi H, Kay MA. Efficient construction of a recombinant adenovirus vector by an improved *in vitro* ligation method. *Hum Gene Ther* 1998; **9**: 2577–2583.
24 Guo ZS, Wang LH, Eisensmith RC, Woo SL. Evaluation of promoter strength for hepatic gene expression *in vivo* following adenovirus-mediated gene transfer. *Gene Ther* 1996; **3**: 802–810.
25 Osaka E, Suzuki T, Osaka S, Yoshida Y, Sugita H, Asami S *et al.* Survivin expression levels as independent predictors of survival for osteosarcoma patients. *J Orthop Res* 2007; **25**: 116–121.
26 Zhang JF, Wei F, Wang HP, Li HM, Qiu W, Ren PK *et al.* Potent anti-tumor activity of telomerase-dependent and HSV-TK armed oncolytic adenovirus for non-small cell lung cancer *in vitro* and *in vivo*. *J Exp Clin Cancer Res* 2010; **29**: 52.
27 Ahn BC, Ronald JA, Kim YI, Katzenberg R, Singh A, Paulmurugan R *et al.* Potent, tumor-specific gene expression in an orthotopic hepatoma rat model using a Survivin-targeted, amplifiable adenoviral vector. *Gene Ther* 2011; **18**: 606–612.
28 White E, Denton A, Stillman B. Role of the adenovirus E1B 19 000-dalton tumor antigen in regulating early gene expression. *J Virol* 1988; **62**: 3445–3454.
29 White E. Regulation of the cell cycle and apoptosis by the oncogenes of adenovirus. *Oncogene* 2001; **20**: 7836–7846.
30 Chang J, Zhao X, Wu X, Guo Y, Guo H, Cao J *et al.* A phase I study of KH901, a conditionally replicating granulocyte–macrophage colony-stimulating factor: armed oncolytic adenovirus for the treatment of head and neck cancers. *Cancer Biol Ther* 2009; **8**: 676–682.
31 Nemunaitis J, Tong AW, Nemunaitis M, Senzer N, Phadke AP, Bedell C *et al.* A phase I study of telomerase-specific replication competent oncolytic adenovirus (telomelysin) for various solid tumors. *Mol Ther* 2010; **18**: 429–434.
32 Messerschmitt PJ, Garcia RM, Abdul-Karim FW, Greenfield EM, Getty PJ. Osteosarcoma. *J Am Acad Orthop Surg* 2009; **17**: 515–527.

Hepatology Research

Hepatology Research 2011; **41**: 594–596 doi: 10.1111/j.1872-034X.2011.00805.x

Letter to the Editor

Recombinant soluble form of heparin-binding epidermal growth factor-like growth factor protein therapy drastically inhibits Fas-mediated fulminant hepatic failure: Implications in clinical application

The mRNA levels of heparin-binding epidermal growth factor-like growth factor (HB-EGF) increased more rapidly than those of hepatocyte growth factor (HGF), the well-studied hepatotropic factor, in regenerating livers after a partial hepatectomy and liver injury.[1–6] The membrane-anchored precursor form (proHB-EGF) is initially synthesized in non-parenchymal cells, and the extracellular domain is cleaved by a specific metalloproteinase.[7,8] The resulting soluble form of HB-EGF (sHB-EGF) acts on neighboring hepatocytes.[1,9] Our previous study demonstrated the therapeutic effects of proHB-EGF gene (pHB-EGFg) therapy in liver disease.[9] The recombinant human sHB-EGF protein (rsHB-EGFp) therapy remains to be studied because it is potentially more clinically suited to inhibit fulminant hepatic failure than pHB-EGFg therapy due to its instant action (i.e. no time lag as in pHB-EGFg therapy, such as proHB-EGF transcription and translation and the subsequent shedding of sHB-EGF in hepatocytes) and the feasibility to terminate treatment, and because the modes of actions may differ between pHB-EGFg and rsHB-EGFp therapies. The present study examines the ability of the rsHB-EGFp therapy to inhibit fulminant hepatic failure in mice.

The initial and essential event in many liver diseases, particularly acute viral hepatitis and the subsequent fulminant hepatic failure, is excessive activation of the Fas system.[4,9,10] Five- to six-week-old male C57BL/6J mice ($n = 8$ per group) were administrated three i.p. injections of 100 μg/mouse rsHB-EGFp at 6 and 0.5 h before and 3 h after the mice were i.p. injected with 4 μg/mouse of an agonistic anti-Fas antibody (4Fas-ip) as previously described.[4,9] Twenty-four hours after administrating 4Fas-ip, the serum alanine aminotransferase (ALT), aspartate aminotransferase (AST) and lactate dehydrogenase (LDH) levels were remarkably increased in the control saline-treated mice (2853 ± 814, 1817 ± 469 and 3782 ± 1222 IU/L, respectively) (Fig. 1a), but were drastically attenuated to normal levels in the rsHB-EGFp-treated mice (ALT, 21 ± 5; AST, 28 ± 4; LDH, 119 ± 16 IU/L). Accordingly, all of the control mice had histopathological liver injury, including apoptosis, while none of the rsHB-EGFp-treated mice had histopathological findings of liver injury 24 h after 4Fas-ip was administrated (Fig. 1b,c). rsHB-EGFp treatment significantly reduced Bax expression, whereas Bcl-2 or Bcl-xl expression was unaffected (Fig. 1d). Because Bax and Bcl-2/Bcl-xl positively and negatively regulate apoptosis, respectively, this result further suggests that rsHB-EGFp therapy ameliorated apoptotic properties.

In survival analyses, four of six (67%) control mice died within 17 h, and only two of six (33%) mice survived up to 48 h after they had received 8 μg/mouse of Fas-ip (8Fas-ip) (Fig. 1e). In contrast, all rsHB-EGFp-treated mice survived up to 48 h after receiving 8Fas-ip.

Our findings and the previous studies revealed that rsHB-EGFp pharmacotherapy elicited greater protective effects than hepatic pHB-EGFg therapy in inhibiting fulminant hepatic failure, because the latter greatly but not completely attenuated liver injury.[9] This difference may be due to the lack of vector-related hepatotoxicity and to direct actions in rsHB-EGFp therapy. Although additional studies should be performed, these promising results and the lack of effective medicines that radically inhibit fulminant hepatic failure indicate that

Correspondence: Dr Ken-ichiro Kosai, Department of Gene Therapy and Regenerative Medicine, Kagoshima University Graduate School of Medical and Dental Sciences, 8-35-1 Sakuragaoka, Kagoshima, 890-8544, Japan. Email: kosai@m2.kufm.kagoshima-u.ac.jp

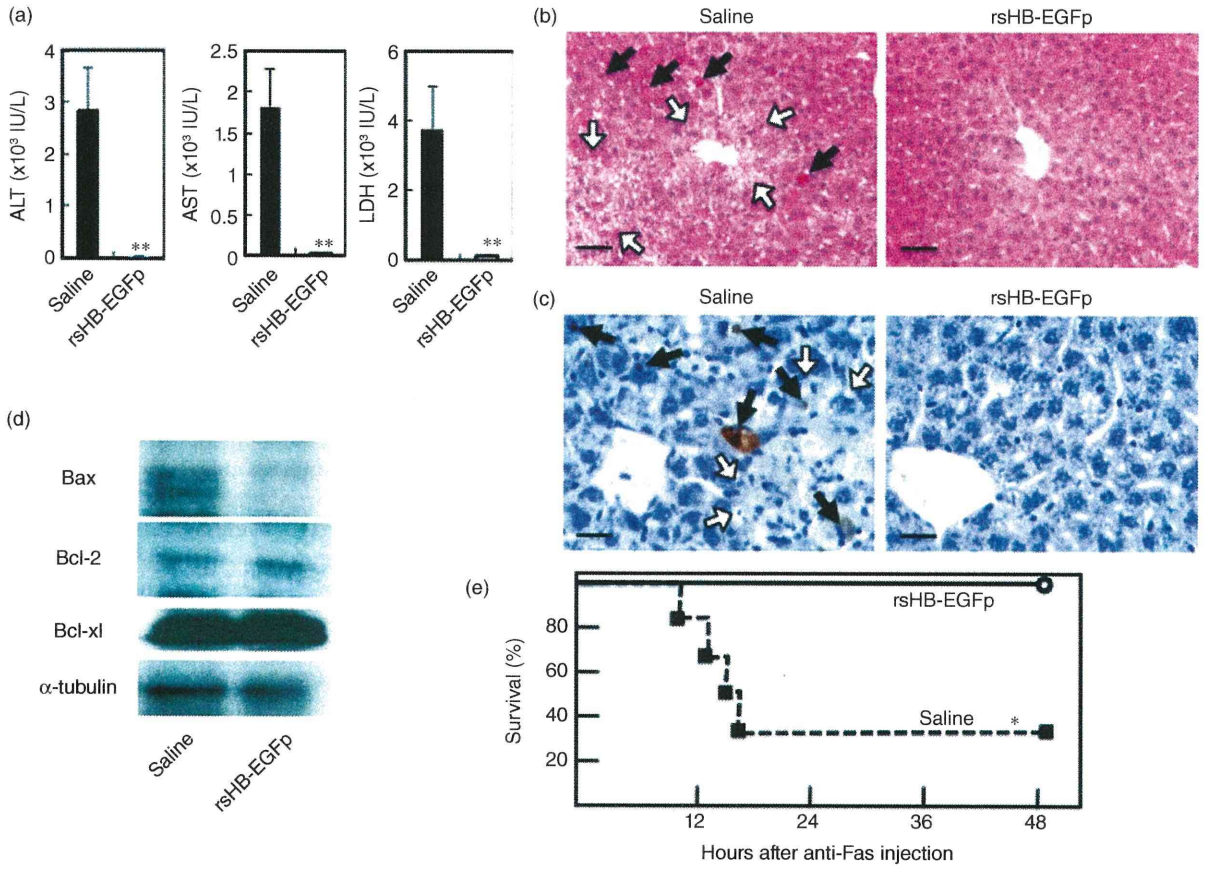

Figure 1 Therapeutic effects of recombinant human soluble form of heparin-binding epidermal growth factor-like growth factor protein (rsHB-EGFp) pharmacotherapy in inhibiting Fas-mediated fulminant hepatic failure in mice. Mice were administrated 4 μg/mouse of an agonistic anti-Fas antibody i.p. (4Fas-ip) (a–d) or 8 μg/mouse of an agonistic anti-Fas antibody i.p. (8Fas-ip) (e) at 0 h and i.p. injections of rsHB-EGFp or saline at –6, –0.5 and 3 h. (a) The serum alanine aminotransferase (ALT), aspartate aminotransferase (AST) and lactate dehydrogenase (LDH) levels at 24 h after 4Fas-ip were drastically increased in the saline-treated control mice, but were virtually normal in the rsHB-EGFp-treated mice. All data are expressed as the mean ± standard error (**$P < 0.01$). (b) Hematoxylin–eosin-stained liver histology sections of the rsHB-EGFp-treated or saline-treated mice 24 h after was administrated 4Fas-ip (scale bar, 100 μm). Histopathological findings of liver injury (e.g. apoptosis [black arrows] and swollen hepatocytes [white arrows]) were observed in the saline-treated mice but not in the rsHB-EGFp-treated mice. (c) Terminal deoxynucleotidyl transferase-mediated deoxyuridine triphosphate nick end labeling (TUNEL)-positive apoptotic cells (black arrows) and clusters of dead hepatocytes (white arrows) were conspicuously found only in the saline-treated mice (scale bar, 50 μm). (d) Western blot analysis of Bax, Bcl-2, Bcl-xl and α-tubulin (internal control) in liver tissues from saline-treated or rsHB-EGFp-treated mice 24 h after 4Fas-ip was administrated. (e) A Kaplan–Meier analysis showed survival differences between the two groups ($n = 6$ per group) (*$P < 0.05$), and all of the rsHB-EGFp-treated mice survived up to 48 h after receiving 8Fas-ip.

rsHB-EGFp pharmacotherapy should be rapidly developed as a clinical therapy.

Ngin Cin Khai,[1] Kouichi Sakamoto,[1,2] Hideo Takamatsu,[3] Hiroshi Matsufuji[2] and Ken-ichiro Kosai[1]

Departments of [1]Gene Therapy and Regenerative Medicine and [2]Pediatric Surgery, Kagoshima University Graduate School of Medical and Dental Science, and [3]Kagoshima University Medical and Dental Hospital, Kagoshima, Japan

REFERENCES

1 Kiso S, Kawata S, Tamura S *et al.* Expression of heparin-binding EGF-like growth factor in rat liver injured by carbon tetrachloride or d-galactosamine. *Biochem Biophys Res Commun* 1996; **220:** 285–8.
2 Kiso S, Kawata S, Tamura S *et al.* Role of heparin-binding epidermal growth factor-like growth factor as a hepatotrophic factor in rat liver regeneration after partial hepatectomy. *Hepatology* 1995; **22:** 1584–90.
3 Kosai K, Matsumoto K, Funakoshi H, Nakamura T. Hepatocyte growth factor prevents endotoxin-induced lethal hepatic failure in mice. *Hepatology* 1999; **30:** 151–9.
4 Kosai K, Matsumoto K, Nagata S, Tsujimoto Y, Nakamura T. Abrogation of Fas-induced fulminant hepatic failure in mice by hepatocyte growth factor. *Biochem Biophys Res Commun* 1998; **244:** 683–90.
5 Kosai KI, Finegold MJ, Thi-Huynh BT *et al.* Retrovirus-mediated in vivo gene transfer in the replicating liver using recombinant hepatocyte growth factor without liver injury or partial hepatectomy. *Hum Gene Ther* 1998; **9:** 1293–301.
6 Ido A, Moriuchi A, Marusawa H *et al.* Translational research on HGF: a phase I/II study of recombinant human HGF for the treatment of fulminant hepatic failure. *Hepatol Res* 2008; **38:** S88–S92.
7 Kimura R, Iwamoto R, Mekada E. Soluble form of heparin-binding EGF-like growth factor contributes to retinoic acid-induced epidermal hyperplasia. *Cell Struct Funct* 2005; **30:** 35–42.
8 Higashiyama S. Metalloproteinase-mediated shedding of heparin-binding EGF-like growth factor and its pathophysiological roles. *Protein Pept Lett* 2004; **11:** 443–50.
9 Khai NC, Takahashi T, Ushikoshi H *et al.* In vivo hepatic HB-EGF gene transduction inhibits Fas-induced liver injury and induces liver regeneration in mice: a comparative study to HGF. *J Hepatol* 2006; **44:** 1046–54.
10 Oksuz M, Akkiz H, Isiksal YF *et al.* Expression of Fas antigen in liver tissue of patients with chronic hepatitis B and C. *Eur J Gastroenterol Hepatol* 2004; **16:** 341–5.

Biochemical and Biophysical Research Communications 413 (2011) 128–135

Contents lists available at SciVerse ScienceDirect

Biochemical and Biophysical Research Communications

journal homepage: www.elsevier.com/locate/ybbrc

Targeting CD9 produces stimulus-independent antiangiogenic effects predominantly in activated endothelial cells during angiogenesis: A novel antiangiogenic therapy

Taro Kamisasanuki [a,b], Saori Tokushige [a], Hiroto Terasaki [a,b], Ngin Cin Khai [a,1], Yuqing Wang [a], Taiji Sakamoto [b], Ken-ichiro Kosai [a,*]

[a] Department of Gene Therapy and Regenerative Medicine, Kagoshima University Graduate School of Medical and Dental Sciences, 8-35-1 Sakuragaoka, Kagoshima 890-8544, Japan
[b] Department of Ophthalmology, Kagoshima University Graduate School of Medical and Dental Sciences, 8-35-1 Sakuragaoka, Kagoshima 890-8544, Japan

ARTICLE INFO

Article history:
Received 5 August 2011
Available online 22 August 2011

Keywords:
Angiogenesis
Tetraspanin
RNAi
VEGF (vascular endothelial growth factor)
HGF (hepatocyte growth factor)
Ocular disease

ABSTRACT

The precise roles of tetraspanin CD9 are unclear. Here we show that CD9 plays a stimulus-independent role in angiogenesis and that inhibiting CD9 expression or function is a potential antiangiogenic therapy. Knocking down CD9 expression significantly inhibited *in vitro* endothelial cell migration and invasion induced by vascular endothelial growth factor (VEGF) or hepatocyte growth factor (HGF). Injecting CD9-specific small interfering RNA (siRNA-CD9) markedly inhibited HGF- or VEGF-induced subconjunctival angiogenesis *in vivo*. Both results revealed potent and stimulus-independent antiangiogenic effects of targeting CD9. Furthermore, intravitreous injections of siRNA-CD9 or anti-CD9 antibodies were therapeutically effective for laser-induced retinal and choroidal neovascularization in mice, a representative ocular angiogenic disease model. In terms of the mechanism, growth factor receptor and downstream signaling activation were not affected, whereas abnormal localization of integrins and membrane type-1 matrix metalloproteinase was observed during angiogenesis, by knocking down CD9 expression. Notably, knocking down CD9 expression did not induce death and mildly inhibited proliferation of quiescent endothelial cells under conditions without an angiogenic stimulus. Thus, CD9 does not directly affect growth factor-induced signal transduction, which is required in angiogenesis and normal vasculature, but is part of the angiogenesis machinery in endothelial cells during angiogenesis. In conclusion, targeting CD9 produced stimulus-independent antiangiogenic effects predominantly in activated endothelial cells during angiogenesis, and appears to be an effective and safe antiangiogenic approach. These results shed light on the biological roles of CD9 and may lead to novel antiangiogenic therapies.

1. Introduction

Angiogenesis is essential for not only organ growth and development in fetuses but also such physiologic processes as tissue homeostasis in adults [1]. Dysregulated angiogenesis contributes to the pathogenesis of many diseases, including several ocular disorders (e.g., diabetic retinopathy, retinopathy of prematurity, age-related macular degeneration), solid tumor growth and/or metastasis, rheumatoid arthritis, and psoriasis [1]. Angiogenesis requires endothelial cells to sprout, migrate, and proliferate and to degrade the extracellular matrix and basement membrane before invasion [2].

Although a variety of molecules are involved in these complex multistep processes, angiogenic growth factors have been implicated as the predominant determinants of angiogenic phenotypes [3]. Particularly, the potent angiogenic activities of vascular endothelial growth factor (VEGF), hepatocyte growth factor (HGF), basic fibroblast growth factor (bFGF), and heparin-binding epidermal growth factor-like growth factor (HB-EGF) have been extensively studied [3–5]. Moreover, the therapeutic effectiveness of anti-VEGF agents for cancer and ocular diseases has been recently shown in experiments and clinical studies, highlighting the importance of angiogenesis and the promise of antiangiogenic therapy [6]. For instance, clinical studies examining neovascular age-related

Abbreviations: VEGF, vascular endothelial growth factor; HGF, hepatocyte growth factor; siRNA-CD9, CD9-specific small interfering RNA; bFGF, basic fibroblast growth factor; HB-EGF, heparin-binding epidermal growth factor-like growth factor; HMVECs, normal adult human dermal microvascular endothelial cells; siRNA-LaminA/C, lamin A/C-specific siRNA; siRNA-Random, control siRNA; TUNEL, terminal deoxynucleotidyl transferase dUTP nick end labeling; FAK, focal adhesion kinase; PBS, phosphate-buffered saline; CNV, choroidal neovascularization.

* Corresponding author. Fax: +81 99 265 9721.
E-mail address: kosai@m2.kufm.kagoshima-u.ac.jp (K.-i. Kosai).
[1] Present address: International Medical School, Management and Science University, Malaysia.

0006-291X/$ - see front matter © 2011 Elsevier Inc. All rights reserved.
doi:10.1016/j.bbrc.2011.08.068

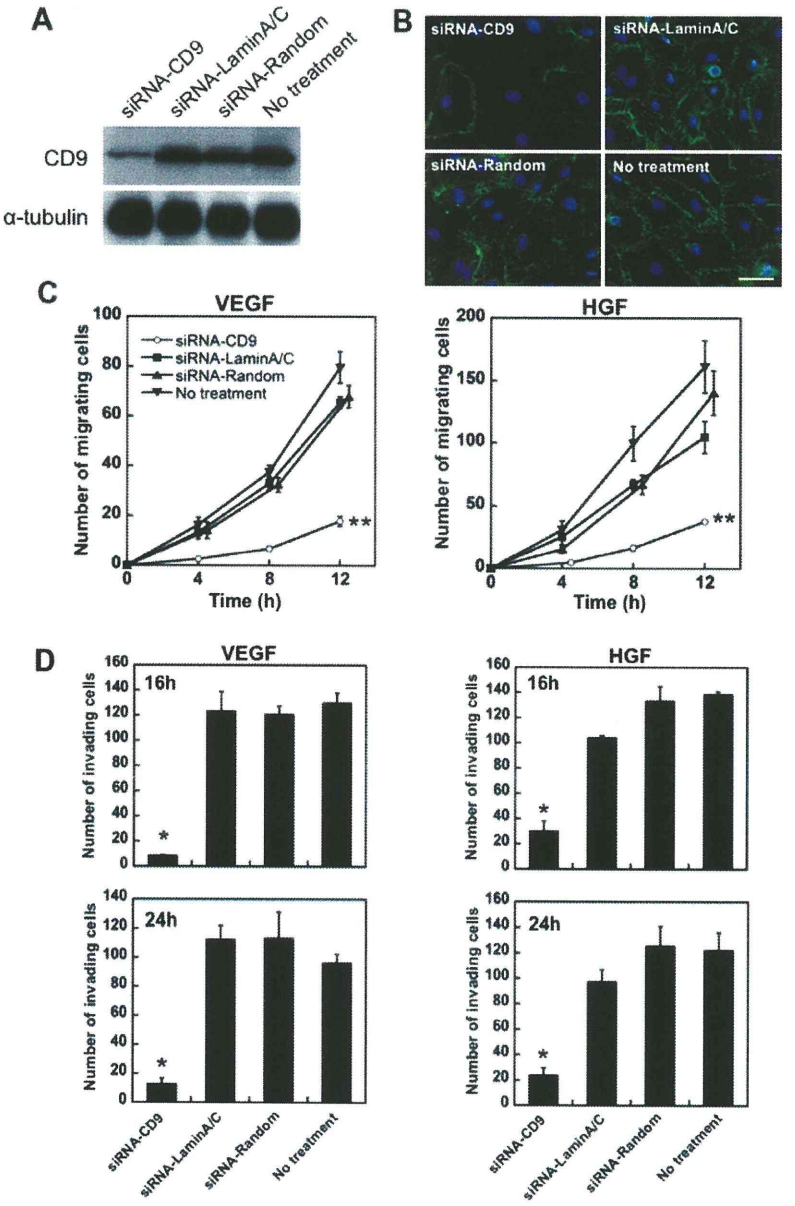

Fig. 1. Knocking down CD9 expression inhibited endothelial cell migration and invasion *in vitro*. (A) Western blot analysis. (B) Immunocytochemical analysis. CD9 protein expression was inhibited by siRNA-CD9. Scale bar, 50 μm. (C, D) Migration (C) and invasion (D) of siRNA-transfected HMVECs through chamber filters and Matrigel-coated membrane filters, respectively, at the indicated time points after treatment with VEGF or HGF. Transfection with siRNA-CD9 significantly inhibited migration and invasion of HMVECs. Results are shown as means ± SEM. $n = 5$ (C) and $n = 3$ in three experiments (D); $^{*}P < 0.05$ and $^{**}P < 0.005$ compared with siRNA-Random (Student's t-test).

macular degeneration revealed more meaningful improvements with intravitreous injections of ranibizumab (anti-VEGF-A antibody) than that with conventional photodynamic therapy [6]. Despite the promising clinical results, anti-VEGF agents do have some limitations as antiangiogenic therapies. Anti-VEGF antibodies, for example, are unlikely to inhibit all VEGF subtypes and receptor families, and clearly do not directly address angiogenesis that is induced by other growth factors, such as HGF [4,5]. Moreover, clinical studies showed that the effectiveness of anti-VEGF antibodies diminished during long-term treatment, and anti-VEGF pharmacotherapy was associated with significant adverse effects, likely owing to responses in normal vessels [7,8]. Rather, an ideal antiangiogenic agent would be easily administered, inhibitory to angiogenesis induced by a range of stimuli, and free of significant safety concerns.

CD9 is a tetraspanin that forms multimolecular complexes via lateral associations with various membrane proteins [9]. Although CD9 has been implicated in cell morphology, motility, and fusion, the precise *in vivo* functions of CD9 have yet to be elucidated [9]. In fact, recent studies of CD9 knockout mice, including experiments performed in several laboratories, identified only an essential role in gamete membrane fusion as a nonredundant function of CD9, even though CD9 is expressed in a range of tissues, including Schwann cells, platelets, smooth muscle cells, and endothelial cells [10,11]. In addition, CD9 was independently cloned as a motility-related protein that may inhibit cancer cell metastasis [12]; the antimetastatic activity remains controversial, however, owing to inconsistent and at times contradicting results, which may reflect differences in the examined cancer types [13,14].

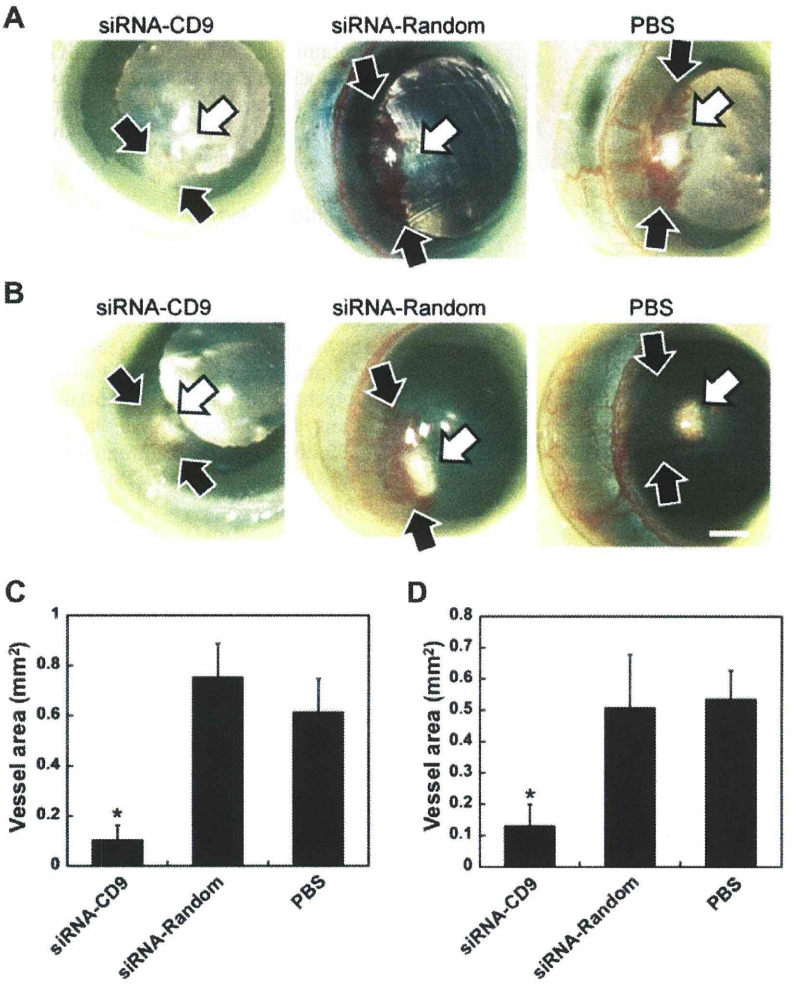

Fig. 2. Injections of siRNA-CD9 efficiently inhibited *in vivo* angiogenesis induced by various stimuli in rat cornea. (A, B) Macroscopic images of neovascularization in rat cornea 7 days after insertion of slow-releasing VEGF (A) or HGF (B) pellets into rat corneal micropockets and subsequent subconjunctival injections of siRNA at 0 and 24 h. White and black arrows indicate inserted pellets and neovascularization, respectively. Scale bar, 1 mm. (C, D) Vessel lengths (C; VEGF, D; HGF) were measured on days 4 and 7, and angiogenic areas were calculated as described in the methods. Results are shown as means ± SEM. $n = 7–10$ in each group. $^*P < 0.05$ versus siRNA-Random (Student's t-test).

We hypothesized that downregulating CD9 expression in endothelial cells during active angiogenesis would reveal the role of CD9, which would be inconspicuous in relatively quiescent endothelial cells. Here, we show that CD9 is stimulus-independently required for angiogenesis *in vitro* and *in vivo*, and demonstrate that a relatively simple injection of CD9-specific small-interfering RNA (siRNA-CD9) was beneficial in a representative ocular angiogenesis disease model.

2. Materials and methods

2.1. Cell culture

Normal adult human dermal microvascular endothelial cells (HMVECs) (Cambrex, East Rutherford, NJ) were cultured in EGM®-2-MV BulletKit® media (Takara Bio, Otsu, Shiga, Japan) according to the manufacturer's protocol except that serum concentrations were reduced from the standard 5% to 2%.

2.2. siRNA transfection

HMVECs were transfected with siRNA-CD9 (the sequence for silencing CD9; sense: 5′-GAGCAUCUUCGAGCAAGAAtt-3′; antisense: 5′-UUCUUGCUCGAAGAUGCUCtt-3′) [15]; lamin A/C-specific siRNA (siRNA-LaminA/C) (sense: 5′-CUGGACUUCCAGAAGAACAtt-3′; anti-sense: 5′-UGUUCUUCUGGAAGUCCAGtt-3′) [16]; or control siRNA (siRNA-Random) (sense: 5′-UCUUAAUCGCGUAUAAGGCtt-3′; antisense: 5′-GCCUUAUACGCGAUUAAGAtt-3′) using Lipofectamine RNAiMAX® and Opti-MEM® (Invitrogen, Carlsbad, CA).

2.3. Migration and invasion assays

For migration and invasion assays, siRNA-transfected HMVECs were plated in media on the upper chamber containing uncoated or Matrigel-coated membrane filters (8.0-μm pore size; Becton Dickinson, Tokyo, Japan). Recombinant VEGF, or HGF (final concentration, 20 ng/mL) was added to the lower chamber. After incubation for the indicated period, the numbers of migrating and invading cells were counted as described previously [17].

2.4. Viability assays

Cell viability was determined using a WST-8 assay as described previously [18,19].

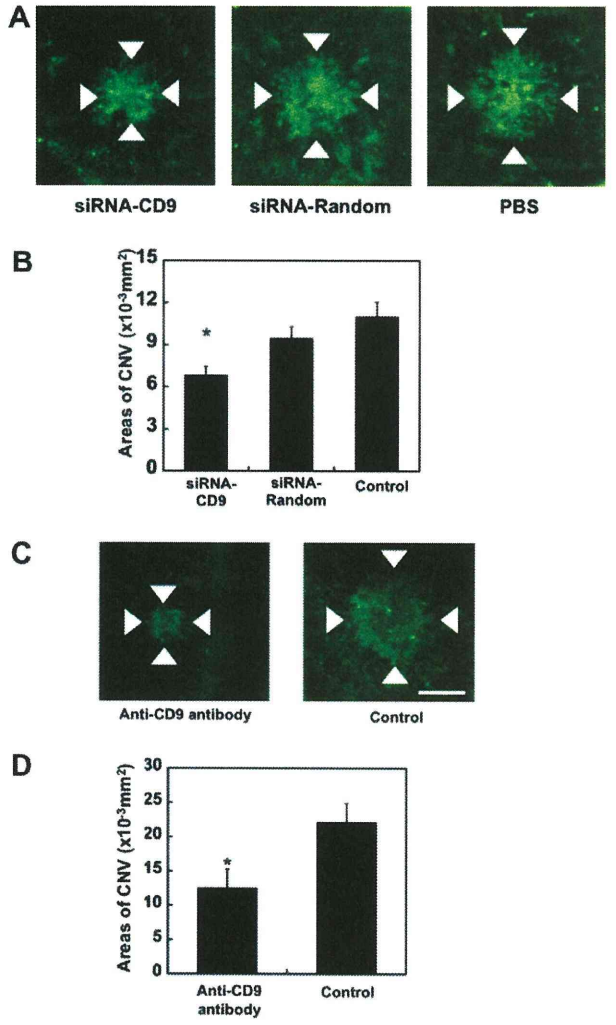

Fig. 3. Intravitreous injections of siRNA-CD9 or anti-CD9 antibodies effectively inhibited CNV. (A, C) Fluorescence images after laser photocoagulation and subsequent siRNA injections (A) or anti-CD9 antibodies (C). Ruptures in Bruch's membrane were induced at 4–5 locations in each eye on day 1. (A) On days 1 and 7, the mice received 3 μL (20 pmol/μL) intravitreous injections of siRNA or PBS in the eyes. On day 14, the mice were perfused with fluorescein-labeled dextran and choroidal flat mounts were examined using fluorescence microscopy. Original magnification, 200×. (C) The same experiment was performed using 5 μL (10 ng) of anti-CD9 antibodies instead of siRNA. Scale bar, 100 μm. Arrowheads in (A, C) indicate areas of CNV. (B, D) Areas of CNV on day 14 as shown in (A, C) were measured. Injections of siRNA-CD9 or anti-CD9 antibodies resulted in significantly smaller areas of CNV than those observed in control samples. Results are shown as means ± SEM. $n = 14–17$ in each group. *$P < 0.05$ siRNA-CD9 versus siRNA-Random, and anti-CD9 antibodies versus control (Student's t-test).

2.5. Immunocytochemistry and terminal deoxynucleotidyl transferase dUTP nick end labeling (TUNEL) staining

Immunocytochemical analysis was performed as described previously [20,21] using either primary anti-CD9 (ALB6, Immunotech by Beckman Coulter, Brea, CA) or anti-Ki-67 (Abcam, Tokyo, Japan) antibodies, fluorescent secondary antibodies (Alexa 488 and/or 594, Invitrogen) and Hoechst 33342 (Invitrogen). TUNEL staining was performed as described previously [19,21].

2.6. In vitro wound healing assay

Wound healing assays were performed as described previously with some modifications [22]. Briefly, monolayers of siRNA-transfected HMVECs on fibronectin-coated slides were disrupted with a pipette tip and subsequently cultured in media containing 20 ng/mL VEGF for 24 h. Lesions were fixed and immunocytochemically labeled with rabbit anti-human MMP14 (MT1-MMP) (Abcam) or rabbit anti-human integrin β1 (Millipore, Tokyo, Japan) antibodies. Secondary anti-rabbit fluorescent antibodies were used for visualization.

2.7. Immunoblotting

Western blot analysis was performed as described previously [19,20] using the following antibodies: anti-CD9 (MM2/57, Southern Biotech, Birmingham, AL), anti-α-tubulin (Sigma–Aldrich, Tokyo, Japan), anti-Flk-1 (Santa Cruz Biotechnology, Santa Cruz, CA), anti-Met (Santa Cruz Biotechnology), anti-FAK (Santa Cruz Biotechnology), anti-phospho-Flk-1 (Tyr951 and Tyr1175, Cell Signaling Technology, Tokyo, Japan), anti-phospho-Met (Tyr1234/1235 and Tyr1349, Cell Signaling Technology; Tyr1356, Abcam), and anti-phospho-FAK (Tyr397, Invitrogen; Tyr925, Santa Cruz Biotechnology).

2.8. Animal experiments

To analyze *in vivo* angiogenic activities, a rat corneal micropocket assay was performed as described previously [23]. Briefly, pellets containing VEGF or HGF (160 ng per pellet) were inserted into surgically created superficial corneal micropockets of 9- to 10-week-old male brown Norway rats (Kyudo, Fukuoka, Japan) on day 1. siRNA in phosphate-buffered saline (PBS; 120 pmol/10 μL per eye) was subconjunctivally injected 1 mm behind the limbus 6 h and 24 h after VEGF or HGF pellet implantation. On days 4 and 7, the lengths of the vessels were measured, and the angiogenic area (mm^2) was calculated according to the following formula: $0.02\pi \times$ vessel length (mm) × hour.

To assess the therapeutic potential of this approach in angiogenic diseases, a choroidal neovascularization (CNV) model was employed as described previously [24]. Briefly, each retina of 7- to 8-week-old male C57BL/6J mice was subjected to 659-nm diode laser photocoagulation to generate burns. Later on the same day (day 1) and on day 7, mice were given intravitreous injections of 2 μL (20 pmol/μL) of siRNA-CD9, siRNA-Random, or PBS alone. Mice were perfused with fluorescein-labeled dextran (Sigma, Aldrich) and sacrificed 14 days after laser photocoagulation. The eyes were removed and flat mounts were examined under a fluorescence microscope. The strongly labeled area associated with each burn, which represented the total fibrovascular scar, was measured.

The protocol for the animal experiments was approved by the Animal Research Committee of Kagoshima University and animal experiments were performed in accordance with NIH Guidelines for the Care and Use of Laboratory Animals.

2.9. Statistical analysis

Data are represented as means ± standard errors. Statistical analysis between test and control groups was performed using Student's t-tests, and $P < 0.05$ was defined as statistical significance.

3. Results

3.1. Migration-inducing activities of angiogenic factors and adenoviral CD9 transduction

After screening four representative angiogenic growth factors—i.e., VEGF, HGF, bFGF and HB-EGF—we chose VEGF and HGF as

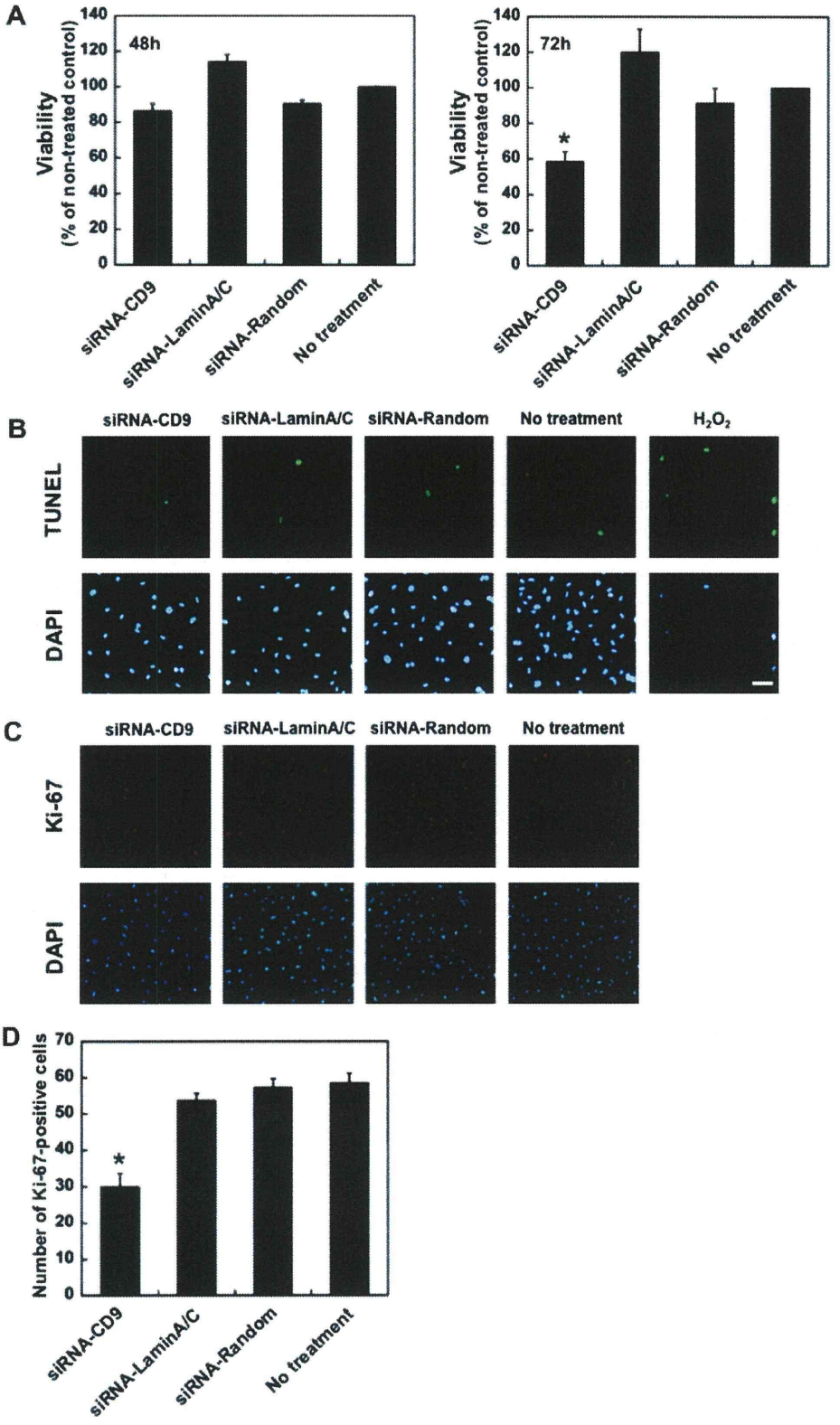

Fig. 4. CD9 is involved in endothelial cell proliferation under physiologic conditions. (A) HMVECs were counted in a WST-8 assay 48 and 72 h after siRNA transfection and subsequent culture without angiogenic stimuli. Knocking down CD9 expression resulted in a significant decrease in the cell number at 72 h but not at 48 h. Results are shown as means ± SEM. $n = 6$ in each group. $^{*}P < 0.05$ versus siRNA-Random (Student's t-test). (B) TUNEL-staining at 72 h using the same experimental conditions described in (A). The number of TUNEL-positive, apoptotic HMVECs did not significantly differ among the treatment groups. Hydrogen peroxide (H_2O_2) was used as a positive control to produce TUNEL-positive apoptotic cells. Scale bar, 100 μm. (C) Fluorescence images of Ki-67-immunocytochemical staining at 72 h using the same experimental condition shown in (A). (D) Ki-67-positive cells were counted in 60 fields under 200× magnification (as shown in (C)). Results are shown as means ± SEM. $n = 12$ for each group. $^{*}P < 0.05$ versus siRNA-Random (Student's t-test).

diverse angiogenic stimuli and used them in the following experiments (Supplementary Fig. S1).

We detected high levels of endogenous CD9 protein in HMVECs, and markedly increased expression was not observed following adenoviral CD9 gene transduction (Supplementary Fig. S2).

3.2. Stimulus-independent inhibition of in vitro migration and invasion by knocking down CD9 expression

We examined whether knockdown of CD9 expression affected *in vitro* HMVEC migration and invasion of using CD9-specific siRNA sequence. Western blotting and immunocytochemical analyses demonstrated that transduction of siRNA-CD9 potently inhibited CD9 expression (Fig. 1A and B). Transduction of siRNA-CD9 significantly inhibited both VEGF- and HGF-induced migration and invasion of endothelial cells (Fig. 1C and D).

3.3. Stimulus-independent inhibition of in vivo angiogenesis by injecting siRNA-CD9

We then examined whether the stimulus-independent antiangiogenic effects of reduced CD9 expression manifest *in vivo* using a rat cornea micropocket angiogenesis assay. With either control injection, both VEGF and HGF induced prominent neovascularization in the avascular corneas after 7 days (Fig. 2A and B). The average neovascular areas in rats administered VEGF or HGF followed by siRNA-CD9 injections were >70% smaller compared with results obtained with control injections (Fig. 2C and D). Our *in vivo* and *in vitro* results demonstrated that knocking down CD9 expression had potent antiangiogenic effects, which were not specific to the stimulus that was used to induce angiogenesis.

3.4. Therapeutic effect of injection of siRNA-CD9 or anti-CD9 antibodies in an eye disease model

We assessed the therapeutic potential of intravitreous injections of siRNA-CD9 using a laser-induced CNV model. Advantages of this animal model include the involvement of a number of factors and a location at which many human ocular angiogenic diseases occur [24]. On day 14, the areas of CNV were 28% and 38% smaller in eyes treated with siRNA-CD9 than in eyes treated with siRNA-Random and vehicle, respectively; these differences were statistically significant (Fig. 3A and B). To further verify the biological finding and to examine the possibility of other therapeutic options, the same experiment was performed using anti-CD9 antibodies rather than siRNA-CD9. The antiangiogenic effects of injections of anti-CD9 antibodies were significant (Fig. 3C and D). Thus, relatively simple interventions, regardless of inhibiting CD9 expression or function, resulted in significant therapeutic effects in an animal disease model. These results further support the crucial role of CD9 in angiogenesis and suggest that various anti-CD9 agents may be clinically effective as antiangiogenic pharmacotherapies.

3.5. Effects of CD9 expression knockdown on activation of growth factor receptors

We examined two possible mechanisms of antiangiogenic effects of targeting CD9. We first analyzed a speculation, whether knocking down CD9 expression affected the activation of growth factor receptors or intercellular signal transduction *in vitro*. Following VEGF stimulation, no significant differences were detected among the groups in VEGF receptor-2 expression levels or activation of this receptor at two well-known phosphorylation sites (Tyr951 and Tyr1175) [4] (Supplementary Fig. 3A). Similarly, expression levels and activation of c-Met/HGF receptors (Tyr1234/1235, Tyr1349 and Tyr1356) [5] following HGF stimulation were not affected by knocking down CD9 expression (Supplementary Fig. 3B). In addition, expression and activation of focal adhesion kinase (FAK), a key mediator of crosstalk between integrin and growth factor receptors [25], were not affected by knocking down CD9 expression (Supplementary Fig. 3A and B). These results suggest that the antiangiogenic effect of targeting CD9 expression is not caused by direct inhibition of angiogenic signaling pathways.

3.6. Abnormal localization of integrins and membrane type 1-matrix metalloproteinase by knocking down CD9 expression

To examine another speculation that CD9 actively functions in the angiogenesis machinery of endothelial cells, the expression and localization of integrin $\alpha 3\beta 1$ and membrane type 1-matrix metalloproteinase (MT1-MMP) were examined by a Western blotting analysis and in an *in vitro* wound healing assay. These proteins were selected because both are involved in angiogenesis and are directly associated with CD9 in some types of cancer [9]. The expression levels of integrin $\alpha 3$ and $\beta 1$ were not affected by knocking down CD9 expression (Supplementary Fig. 4). Reduced CD9 expression, however, resulted in abnormal localization of integrin $\beta 1$ and MT1-MMP and accumulation of both proteins at membrane leading edge in migrating cells at the wound border (*Supplementary* Fig. 4B–D). Thus, CD9 appears to, at least in part, contribute to the delocalization of integrins and MT1-MMP, disruption of which may prevent angiogenesis.

3.7. The roles of CD9 in relatively quiescent endothelial cells

To examine the roles of CD9 in relatively quiescent rather than actively stimulated endothelial cells, changes in viable cell numbers in response to reduced CD9 expression without an angiogenic stimulus were examined *in vtiro*. Significantly fewer cells were present 72 h but not 48 h after transduction of siRNA-CD9 compared with results obtained with any of the control samples (siRNA-LaminA/C, siRNA-random, and no siRNA) (Fig. 4A). Because these results may have reflected induction of cell death or inhibition of cell growth, we assessed the samples using TUNEL and immunocytochemistry for Ki-67. The number of TUNEL-positive apoptotic cells was not affected by knocking down CD9 expression, suggesting that CD9 is not an angiotrophic factor that is essential for endothelial cell survival (Fig. 4B). In contrast, the number of Ki-67-positive proliferating cells decreased in response to siRNA-CD9 (Fig. 4C and D). Thus, CD9 is involved in the proliferation but not survival of relatively quiescent endothelial cells, although knocking down CD9 expression under these conditions produced a phenotype that was less severe than that detected during angiogenesis.

4. Discussion

This is the first study to elucidate that targeting CD9 can be an effective and stimulus-independent antiangiogenic medicine, at least for ocular diseases, and has provided clinically and biologically meaningful information. Interestingly, CD9 plays a critical stimulus-independent and predominant role in activated rather than quiescent endothelial cells. In contrast to its significant contribution to angiogenesis, CD9 showed a lesser role in the proliferation but not survival of endothelial cells under quiescent conditions. Although a previous study showed an association between CD9 and growth factor receptors in cancer [26], the phenotype observed in our study suggested that CD9 does not interact directly with growth factor receptors to transduce angiogenic

signals in endothelial cells. In this regard, it should be noted that both integrin β1 and MT1-MMP were abnormally localized at the leading edge of the lesion following knock down of CD9 expression. CD9 colocalizes and/or associates on membranes with integrins, particularly integrin α3β1 in endothelial cells, and integrins themselves are critically involved in angiogenesis [27]. Similarly, MT1-MMP contributes to angiogenesis by associating with actin fibers in the lamellipodia of migrating cells where it performs proteolytic functions and by internalization of MT1-MMP via caveolae [28]. On the other hand, cellular delocalization of integrins and MT1-MMP is essential for cell migration and/or invasion [29]. In this respect, our findings suggest that CD9, unlike VEGF, is not an angiotrophic factor that is required for endothelial cell survival, but is instead part of the angiogenesis machinery in endothelial cells, mediating migration, proliferation, and degradation of the extracellular matrix during invasion, probably by interacting with other membrane-associated partner proteins, e.g., the delocalization of integrins and MT1-MMP [2,9]. Elucidating the precise underlying molecular mechanisms should be examined in future studies focusing on a number of candidate and/or yet to be identified partner proteins [9].

Clinically, targeting CD9—possibly via simple intravitreous injections of siRNA-CD9 or anti-CD9 antibodies—appears to be an effective, stimulus-independent, and safe antiangiogenic approach. Importantly, stimulus-independent therapy may be superior to specific anti-VEGF agents. Moreover, this method also benefits from the predominant effects during angiogenesis rather than on existing vasculature. Deficiencies identified in clinical applications of bevacizumab (anti-VEGF antibody) include macular ischemia and sustained elevation in intraocular pressure after local intravitreous injections for ocular diseases, and more widespread side effects after systemic injections of bevacizumab for cancer [7,8,30]. These effects are likely caused, at least in part, by roles of VEGF in both angiogenesis and the normal vasculature. On the other hand, siRNA-CD9 and anti-CD9 antibodies may have fewer side effects for a number of reasons. First, unlike anti-VEGF agents, knocking down CD9 expression did not directly inhibit growth factor-induced signal transduction, which is required in normal vasculature and angiogenesis. Second, knocking down of CD9 expression did not induce cell death under conditions in which the cells were relatively quiescent. Third, adult CD9 knockout mice in previous studies did not show marked abnormalities in vasculogenesis or vasculature [10]. These results support our hypothesis that targeting CD9 may have fewer side effects, although this must be carefully studied in future preclinical studies.

In conclusion, the present study revealed that CD9 plays a stimulus-independent role in the angiogenic activity of endothelial cells, and inhibition of CD9 expression or function via intravitreous injections of siRNA-CD9 or anti-CD9 antibodies may provide a new therapeutic strategy for angiogenesis such as that observed in certain ocular diseases.

Acknowledgments

We thank S. Yamashita for technical assistance. This work was supported by a Grant for Promoting Business using Advanced Technology from the Japan Society and Technology Agency, and a Health and Labour Science Research Grants for Third Term Comprehensive Control Research for Cancer from the Ministry of Health, Labour and Welfare of Japan.

Appendix A. Supplementary data

Supplementary data associated with this article can be found, in the online version, at doi:10.1016/j.bbrc.2011.08.068.

References

[1] P. Carmeliet, Angiogenesis in health and disease, Nat. Med. 9 (2003) 653–660.
[2] G.E. Davis, D.R. Senger, Endothelial extracellular matrix: biosynthesis, remodeling, and functions during vascular morphogenesis and neovessel stabilization, Circ. Res. 97 (2005) 1093–1107.
[3] A. Kvanta, Ocular angiogenesis: the role of growth factors, Acta Ophthalmol. Scand. 84 (2006) 282–288.
[4] A.K. Olsson, A. Dimberg, J. Kreuger, L. Claesson-Welsh, VEGF receptor signalling—in control of vascular function, Nat. Rev. Mol. Cell Biol. 7 (2006) 359–371.
[5] W.K. You, D.M. McDonald, The hepatocyte growth factor/c-Met signaling pathway as a therapeutic target to inhibit angiogenesis, BMB Rep. 41 (2008) 833–839.
[6] N.M. Bressler, T.S. Chang, J.T. Fine, C.M. Dolan, J. Ward, Improved vision-related function after ranibizumab vs photodynamic therapy: a randomized clinical trial, Arch. Ophthalmol. 127 (2009) 13–21.
[7] M.Y. Kahook, A.E. Kimura, L.J. Wong, D.A. Ammar, M.A. Maycotte, N. Mandava, Sustained elevation in intraocular pressure associated with intravitreal bevacizumab injections, Ophthalmic Surg. Lasers Imaging 40 (2009) 293–295.
[8] E.J. Sabet-Peyman, F.M. Heussen, J.E. Thorne, H. Casparis, S.J. Patel, D.V. Do, Progression of macular ischemia following intravitreal bevacizumab, Ophthalmic Surg. Lasers Imaging 40 (2009) 316–318.
[9] M.E. Hemler, Targeting of tetraspanin proteins—potential benefits and strategies, Nat. Rev. Drug Discovery 7 (2008) 747–758.
[10] K. Miyado, G. Yamada, S. Yamada, H. Hasuwa, Y. Nakamura, F. Ryu, K. Suzuki, K. Kosai, K. Inoue, A. Ogura, M. Okabe, E. Mekada, Requirement of CD9 on the egg plasma membrane for fertilization, Science 287 (2000) 321–324.
[11] F. Le Naour, E. Rubinstein, C. Jasmin, M. Prenant, C. Boucheix, Severely reduced female fertility in CD9-deficient mice, Science 287 (2000) 319–321.
[12] M. Miyake, M. Koyama, M. Seno, S. Ikeyama, Identification of the motility-related protein (MRP-1), recognized by monoclonal antibody M31-15, which inhibits cell motility, J. Exp. Med. 174 (1991) 1347–1354.
[13] V. Zvieriev, J.C. Wang, M. Chevrette, Over-expression of CD9 does not affect in vivo tumorigenic or metastatic properties of human prostate cancer cells, Biochem. Biophys. Res. Commun. 337 (2005) 498–504.
[14] H. Hori, S. Yano, K. Koufuji, J. Takeda, K. Shirouzu, CD9 expression in gastric cancer and its significance, J. Surg. Res. 117 (2004) 208–215.
[15] O. Barreiro, M. Yanez-Mo, M. Sala-Valdes, M.D. Gutierrez-Lopez, S. Ovalle, A. Higginbottom, P.N. Monk, C. Cabanas, F. Sanchez-Madrid, Endothelial tetraspanin microdomains regulate leukocyte firm adhesion during extravasation, Blood 105 (2005) 2852–2861.
[16] V. Pekovic, J. Harborth, J.L. Broers, F.C. Ramaekers, B. van Engelen, M. Lammens, T. von Zglinicki, R. Foisner, C. Hutchison, E. Markiewicz, Nucleoplasmic LAP2alpha-lamin A complexes are required to maintain a proliferative state in human fibroblasts, J. Cell Biol. 176 (2007) 163–172.
[17] T. Ikoma, T. Takahashi, S. Nagano, Y.M. Li, Y. Ohno, K. Ando, T. Fujiwara, H. Fujiwara, K. Kosai, A definitive role of RhoC in metastasis of orthotopic lung cancer in mice, Clin. Cancer Res. 10 (2004) 1192–1200.
[18] J. Kamizono, S. Nagano, Y. Murofushi, S. Komiya, H. Fujiwara, T. Matsuishi, K. Kosai, Survivin-responsive conditionally replicating adenovirus exhibits cancer-specific and efficient viral replication, Cancer Res. 65 (2005) 5284–5291.
[19] K. Yuge, T. Takahashi, S. Nagano, Y. Terazaki, Y. Murofushi, H. Ushikoshi, T. Kawai, N.C. Khai, T. Nakamura, H. Fujiwara, K. Kosai, Adenoviral gene transduction of hepatocyte growth factor elicits inhibitory effects for hepatoma, Int. J. Oncol. 27 (2005) 77–85.
[20] T. Takahashi, T. Kawai, H. Ushikoshi, S. Nagano, H. Oshika, M. Inoue, T. Kunisada, G. Takemura, H. Fujiwara, K. Kosai, Identification and isolation of embryonic stem cell-derived target cells by adenoviral conditional targeting, Mol. Ther. 14 (2006) 673–683.
[21] N.C. Khai, T. Takahashi, H. Ushikoshi, S. Nagano, K. Yuge, M. Esaki, T. Kawai, K. Goto, Y. Murofushi, T. Fujiwara, H. Fujiwara, K. Kosai, In vivo hepatic HB-EGF gene transduction inhibits Fas-induced liver injury and induces liver regeneration in mice: a comparative study to HGF, J. Hepatol. 44 (2006) 1046–1054.
[22] H. Deissler, E.M. Kuhn, G.E. Lang, Tetraspanin CD9 is involved in the migration of retinal microvascular endothelial cells, Int. J. Mol. Med. 20 (2007) 643–652.
[23] M.S. Rogers, A.E. Birsner, R.J. D'Amato, The mouse cornea micropocket angiogenesis assay, Nat. Protoc. 2 (2007) 2545–2550.
[24] J. Shen, R. Samul, R.L. Silva, H. Akiyama, H. Liu, Y. Saishin, S.F. Hackett, S. Zinnen, K. Kossen, K. Fosnaugh, C. Vargeese, A. Gomez, K. Bouhana, R. Aitchison, P. Pavco, P.A. Campochiaro, Suppression of ocular neovascularization with siRNA targeting VEGF receptor 1, Gene Ther. 13 (2006) 225–234.
[25] E. Sulpice, S. Ding, B. Muscatelli-Groux, M. Berge, Z.C. Han, J. Plouet, G. Tobelem, T. Merkulova-Rainon, Cross-talk between the VEGF-A and HGF signalling pathways in endothelial cells, Biol. Cell 101 (2009) 525–539.
[26] Y. Murayama, Y. Shinomura, K. Oritani, J. Miyagawa, H. Yoshida, M. Nishida, F. Katsube, M. Shiraga, T. Miyazaki, T. Nakamoto, S. Tsutsui, S. Tamura, S. Higashiyama, I. Shimomura, N. Hayashi, The tetraspanin CD9 modulates epidermal growth factor receptor signaling in cancer cells, J. Cell. Physiol. 216 (2008) 135–143.

[27] F. Berditchevski, Complexes of tetraspanins with integrins: more than meets the eye, J. Cell Sci. 114 (2001) 4143–4151.
[28] B.G. Galvez, S. Matias-Roman, M. Yanez-Mo, M. Vicente-Manzanares, F. Sanchez-Madrid, A.G. Arroyo, Caveolae are a novel pathway for membrane-type 1 matrix metalloproteinase traffic in human endothelial cells, Mol. Biol. Cell 15 (2004) 678–687.
[29] A.J. Ridley, M.A. Schwartz, K. Burridge, R.A. Firtel, M.H. Ginsberg, G. Borisy, J.T. Parsons, A.R. Horwitz, Cell migration: integrating signals from front to back, Science 302 (2003) 1704–1709.
[30] T. Kamba, D.M. McDonald, Mechanisms of adverse effects of anti-VEGF therapy for cancer, Br. J. Cancer 96 (2007) 1788–1795.

OPEN ACCESS Freely available online

PLoS one

Suppression of Osteosarcoma Cell Invasion by Chemotherapy Is Mediated by Urokinase Plasminogen Activator Activity via Up-Regulation of EGR1

Yukihiro Matsunoshita[1], Kosei Ijiri[1], Yasuhiro Ishidou[2], Satoshi Nagano[1], Takuya Yamamoto[1], Hiroko Nagao[1], Setsuro Komiya[1], Takao Setoguchi[1]*

1 Department of Orthopaedic Surgery, Graduate School of Medical and Dental Sciences, Kagoshima University, Kagoshima, Japan, **2** Department of Medical Joint Materials, Graduate School of Medical and Dental Sciences, Kagoshima University, Kagoshima, Japan

Abstract

Background: The cellular and molecular mechanisms of tumour response following chemotherapy are largely unknown. We found that low dose anti-tumour agents up-regulate *early growth response 1* (*EGR1*) expression. EGR1 is a member of the immediate-early gene group of transcription factors which modulate transcription of multiple genes involved in cell proliferation, differentiation, and development. It has been reported that EGR1 act as either tumour promoting factor or suppressor. We therefore examined the expression and function of *EGR1* in osteosarcoma.

Methods: We investigated the expression of EGR1 in human osteosarcoma cell lines and biopsy specimens. We next examined the expression of EGR1 following anti-tumour agents treatment. To examine the function of EGR1 in osteosarcoma, we assessed the tumour growth and invasion in vitro and in vivo.

Results: Real-time PCR revealed that *EGR1* was down-regulated both in osteosarcoma cell lines and osteosarcoma patients' biopsy specimens. In addition, EGR1 was up-regulated both in osteosarcoma patient' specimens and osteosarcoma cell lines following anti-tumour agent treatment. Although forced expression of EGR1 did not prevent osteosarcoma growth, forced expression of EGR1 prevented osteosarcoma cell invasion in vitro. In addition, forced expression of EGR1 promoted down-regulation of urokinase plasminogen activator, urokinase receptor, and urokinase plasminogen activity. Xenograft mice models showed that forced expression of EGR1 prevents osteosarcoma cell migration into blood vessels.

Conclusions: These findings suggest that although chemotherapy could not prevent osteosarcoma growth in chemotherapy-resistant patients, it did prevent osteosarcoma cell invasion by down-regulation of urokinase plasminogen activity via up-regulation of EGR1 during chemotherapy periods.

Citation: Matsunoshita Y, Ijiri K, Ishidou Y, Nagano S, Yamamoto T, et al. (2011) Suppression of Osteosarcoma Cell Invasion by Chemotherapy Is Mediated by Urokinase Plasminogen Activator Activity via Up-Regulation of EGR1. PLoS ONE 6(1): e16234. doi:10.1371/journal.pone.0016234

Editor: Ming Tat Ling, Queensland University of Technology, Australia

Received August 7, 2010; **Accepted** December 17, 2010; **Published** January 20, 2011

Funding: This work was supported by Grants-in-Aid for Scientific Research (B) 18390419, (C) 19591725, (C) 20591786, (C) 21591919, (C) 21591920, and (C) 22591663 (KAKENHI), and a Grant-in-Aid from the Ministry of Health, Labour, and Welfare of Japan for the Third Term Comprehensive Control Research for Cancer (http://www.jsps.go.jp/j-grantsinaid/index.html, http://ganjoho.ncc.go.jp/pro/taigan/index.html). The funders had no role in study design, data collection and analysis, decision to publish, or preparation of manuscript.

Competing Interests: The authors have declared that no competing interests exist.

* E-mail: setoro@m2.kufm.kagoshima-u.ac.jp

Introduction

Osteosarcoma is the most frequent primary malignant bone tumor. After initial diagnosis is made by biopsy, treatment consists of preoperative chemotherapy, followed by definitive surgery and postoperative chemotherapy. The Survival rates for patients treated with intensive multidrug chemotherapy and aggressive local control have been reported at 60–80% [1–5]. Indeed, patients with non-metastatic disease have a 70% chance of long-term survival. Eighty percent of patients die of metastatic disease, most commonly in the lungs [3]. Unfortunately, patients with metastatic disease at diagnosis or those who have recurrent disease have a poor prognosis, with only 20% surviving at 5 years, indicating that new therapeutic options for them need to be actively explored [6,7].

The early growth response gene 1 (*EGR1*) is a member of the immediate-early gene group of transcription factors which modulate transcription of multiple genes involved in cell proliferation, differentiation, and development [8]. Expression of *EGR1* is significantly reduced in a number of tumor cells [9,10], and loss of expression of it is closely associated with tumor formation in mammalian cells and tissues [10]. On the other hand, stable expression of *EGR1* inhibited cell proliferation and soft agar growth in NIH3T3 cells transformed with v-*sis*, indicating that *EGR1* functions as a tumor suppressor [11]. We therefore examined the expression and function of *EGR1* in osteosarcoma. Here, we report that expression of *EGR1* is down-regulated in human osteosarcoma cell lines and patient' biopsy specimens. In addition, treatment with anti-tumour agents promoted up-regulation of *EGR1*. Although forced expression of EGR1 did not affect osteosarcoma growth,

forced expression of EGR1 inhibited osteosarcoma cell invasion by down-regulation of urokinase plasminogen activator (uPA) and urokinase receptor (uPAR).

Materials and Methods

Cell culture

143B, Saos-2, HOS, and MG63 cells were purchased from the American Type Culture Collection (ATCC, USA). NOS-1 was provided by the RIKEN BRC through the National Bio-Resource Project of The MEXT, Japan (Tsukuba, Japan) [12]. Cells were grown in Dulbecco's modified Eagle's medium (DMEM) supplemented with 10% FBS, penicillin (100 U/ml), and streptomycin (100 μg/ml). Human osteoblast cells (NHOst) were purchased from Sanko Junyaku (Tokyo, Japan). NHOst was cultured with OBM™ (Cambrex, East Rutherford, NJ, USA) or DMEM supplemented with 10% FBS. All cells were grown in a humidified atmosphere containing 5% CO_2 at 37°C.

Anti-tumor agents

Doxorubicin, methotrexate, and etoposide were purchased from Sigma-Aldrich (MO, USA). Cisplatin was purchased from LKT laboratories (MN, USA).

Patient' specimens

All human osteosarcoma biopsy specimens were obtained from primary lesions. Biopsy was performed before chemotherapy or radio therapy to make the diagnosis. Normal bone tissue was obtained from femur during total hip arthroplasty. Specimens of OS6, OS8, and OS9 tumors were obtained during tumor resection in osteosarcoma patients who received chemotherapy. Doxrubicin, methotrexate, and cisplatin were given to these three patients according to COSS-86 protocol. We compared the EGR1 expressions in the biopsy specimens and the resected tumor specimens obtained from these patients. The study protocol was approved by the institutional review board of the Kagoshima University. All patients and controls gave written informed consent.

Real-time PCR

For real-time PCR, total RNA was obtained 24 h, 48 h, and 5 days following drug treatment. DNase-treated and reverse-transcribed using oligo(dT) primers as described by the manufacturer (Invitrogen, Carlsbad, CA, USA). Reactions were run using SYBR Green (BIO-RAD, Hercules, CA, USA) on a MiniOpticon™ machine (BIO-RAD). The comparative Ct (ΔΔCt) method was used to determine fold change in expression using *GAPDH* or *ACTB*. Each sample was run minimally at three concentrations in triplicate. All primer sets amplified 150- to 200-bp fragments. The primers sequences used were follows: for *EGR1*: 5-CAGCACCTTCAACCCTCAG-3, 5- CACAAGGTGTTGCCACTGTT-3; *uPA*: 5- TGTGAGATCACTGGCTTTGG-3, 5- GTCAGCAGCACACAGCATTT-3; *uPAR*: 5- TGAAGAACAGTGCCTGGATG-3, 5- TGTTGCAGCATTTCAGGAAG-3; *GAPDH*: 5- GAAGGTGAAGGTCGGAGTC-3, 5- GAAGATGGTGATGGGATTTC-3; *ACTB*: 5-AGAAAATCTGGCACCACACC-3, 5-AGAGGCGTACAGGGATAGCA-3.

MTT assay

Following 100 ng–1 μg cisplatin, 1 ng–10 ng methotrexate, 50 ng–1000 ng etoposide, or 10 ng–100 ng doxorubicin treatment, we performed MTT assay to evaluate the osteosarcoma growth as previously reported [13]. In addition, we transfected control vector or EGR1 expression vector, and examined osteosarcoma cell growth by MTT assay. Cells were incubated with substrate for MTT (3-(4,5-dimethylthiazol-2-yl)-2,5-diphenyltetrazolium bromide) for 4 hours, and washed with PBS and lysed to release formazan from cells. Then cells were analyzed in a Safire microplate reader (BIO-RAD) at 562 nm.

Vector transfection

EGR1 expression vector was purchased from Origene (Maryland, USA). EGR1 was cloned into pCMV6-Entry Neomycin Vector. Lipofection of expression vector was performed as recommended in the supplier's protocol using FuGENE 6 (Roche, Basel, Switzerland). All transfected cells were treated with neomycin constitutively to obtain stable transfectants. EGR stable transfectants were used for invasion assay, examinations of uPA and uPAR expressions, and in vivo experiments.

Colony formation assay

Colony formation assay was performed as previously described [14]. Briefly, cells were suspended in DMEM containing 0.33% agar and 10% fetal bovine serum and plated onto the bottom layer containing 0.5% agar. The cells were plated at a density of 5×10^3 per well in a 24-well plate, and colonies were counted 14 days later. Each condition was analyzed in triplicate, and all experiments were repeated three times.

Invasion assay

Invasion of osteosarcoma cells was measured using the BD BioCoat™ BD Matrigel™ Invasion Chamber (BD Bioscience, NJ, U.S.A.) according to the manufacturer's protocol. Briefly, the cells were transfected with plasmids and selected by neomycin. Osteosarcoma cells were seeded onto the membrane of the upper chamber of the transwell at a concentration of $3–5\times10^5$/ml in 2 ml of DMEM medium. The medium in the upper chamber was serum-free. The medium in the lower chamber contained 5% fetal calf serum as a source of chemoattractants. Cells that passed through the Matrigel-coated membrane were stained with Diff-Quik (Sysmex, Kobe, Japan) and photographed.

Western blot

Western blot analysis was performed as previously reported [15]. Briefly, cells were lysed using NP40 lysis buffer (0.5% NP40, 10 mM Tris-HCl (pH 7.4), 150 mM NaCl, 3 mM pAPMSF (Wako Chemicals, Kanagawa, Japan), 5 mg/ml aprotinin (Sigma, StLouis, USA), 2 mM sodium orthovanadate (Wako Chemicals, Kanagawa, Japan), and 5 mM EDTA). Lysates were subjected to SDS-PAGE and subsequent immunoblotting was performed. Following antibodies were used: ant- EGR1 and anti-beta actin (Santa Cruz, CA. U.S.A). Detection was performed using the ECL detection system (Amersham, Giles, UK).

uPA activity assay

uPA activity assay was performed with cell extracts according to the manufacturer's instructions, with absorption measured at 340 nm (Innovative Research, MI, U.S.A.). The assay measures only the active species of uPA, and a standard curve was generated using recombinant active uPA. The assay conditions were optimized so that the amount of tissue extract or cell extract added gave rise to uPA activity within the linear range of detection. Each reaction was performed in triplicate, and all experiments were repeated for three times.

Xenograft model of osteosarcoma

For subcutaneous xenograft models, 143B cells were suspended in 100 μL Matrigel (BD, NJ USA.). Cell suspensions were

subcutaneously inoculated in nude mice. Three weeks after inoculation, 4 μg/kg doxorubicin was administered by intraperitoneal injection. One day after treatment, mice were scarified and tumors were examined. For metastasis experiments, 143B cells (5×10^5) were transfected with GFP lentiviral particles (Santa Cruz, CA. U.S.A). Stably-GFP-expressing 143B cells (1×10^6) were mixed with a collagen gel in a 1:1 volume, and inoculated into the left knee joint of 6-weeks-old nude mice. Five weeks after inoculation, the mice were sacrificed. GFP-positive-143B cells were counted in 50 μl blood aspirates from hearts using the M165 FC microscope (Leica Microsystems, Wild Heerbrugg, Switzerland). Metastatic nodules in the lungs were evaluated by direct microscopic visualization using an M165 FC microscope. Lung metastasis area was calculated by Lumina Vision (Mitani Corporation, Tokyo, Japan). All experimental procedures were performed in compliance with the guiding principles for the Care and Use of Animals described in the American Journal of Physiology and with the Guidelines established by the Institute of Laboratory Animal Sciences, Faculty of Medicine, Kagoshima University (approval number: 20064). All efforts were made to minimize animal suffering, to reduce the number of animals used, and to utilize possible alternatives to in vivo techniques.

ELISA

Expression levels of uPA and uPAR proteins were assayed using specific enzyme-linked immunosorbent assay kits according to the manufacturer's instructions (Abnova, Taipei, Taiwan). Cell lysates were collected by EGR1 stable transfected osteosarcoma cells.

Statistics

Each sample was analyzed in triplicate, and experiments were repeated three times. In all figures, error bars are standard deviations. All statistical analyses were performed using Microsoft Office Excel (Microsoft, Albuquerque, New Mexico, USA) and STASTISCA (StatSoft, Tulsa, OK, USA). Differences between mean values were evaluated by the unpaired *t*-test, and differences in frequencies by Fisher's exact test. Differences were considered significant at $P<0.05$.

Results

EGR1 is down-regulated in osteosarcoma cell lines and patient' specimens

Real-time PCR was performed to examine the gene expression of *EGR1* in osteoblast and osteosarcoma cell lines including NHOst, 143B, Saos-2, HOS, MG63, and NOS-1. Real-time PCR revealed that the 5 of 5 osteosarcoma cell lines exhibited 0.002- to 0.369-fold decreased in expression of *EGR1* (**Figure 1A**). In addition, we performed real-time PCR using patient' biopsy specimens. Real-time PCR revealed that *EGR1* was decreased 0.01-to 0.2-fold in 8 of 10 human biopsy specimens (**Figure 1B**). These findings suggest that the *EGR1* is down-regulated in human osteosarcomas.

Anti-tumour agent treatment promoted up-regulation of *EGR1*

To examine the effects of anti-tumour agents on *EGR1* expression, we performed real-time PCR after anti-tumour agent treatment. We attempt to clarify the changes in EGR1 expression following low-dose anti-tumor agent treatment, and determined anti-tumor drug concentrations required to prevent osteosarcoma cell proliferation. MTT assay revealed that 250 ng/ml cisplatin, 1 ng/ml methotrexate, 50 ng/ml etoposide, or 10 ng/ml doxorubicin treatment did not prevent 143B cell growth. Growth of Saos-2 cells was not inhibited by 1 ng/ml methotrexate, 5 ng/ml methotrexate, 10 ng/ml methotrexate, 50 ng/ml etoposide, or 10 ng/ml doxorubicin. On the other hand, Growth of 143B cell and Saos-2 cell was inhibited by higher dose of each drug (**Figure 2 A, B**). Following 24 h treatment with these concentrations of anti-tumor drugs, *EGR1* was up-regulated (**Figure 3 A–D**). Following 48 h or 5 days treatment, cisplatin, methotrexate, etoposide or doxorubicin increased *EGR1* expression in 143B cell and Saos-2 cells (**Figure S1**). We next examined the expression of *EGR1* following chemotherapy in biopsy specimens. Specimens of OS6, OS8, and OS9 tumors were obtained during tumor resection in osteosarcoma patients who received chemotherapy. We compared the *EGR1* expressions in the biopsy specimens and the resected tumor specimens obtained from these patients. In 3 of 3 patient' specimens examined, *EGR1* expression was increased 7.87- to 1.71 following chemotherapy (**Figure S2A**). To examine the expression of *EGR1* following low-dose chemotherapy in vivo, we used a novel osteosarcoma murine xenograft model with 143B cells. We injected 4 μg/kg doxorubicin which is less than one-hundred dose of COSS-86 protocol for osteosarcoma patients. Real-time PCR showed that low dose doxorubicin treatment promoted up-regulation of *EGR1* in vivo (**Figure S2B**).

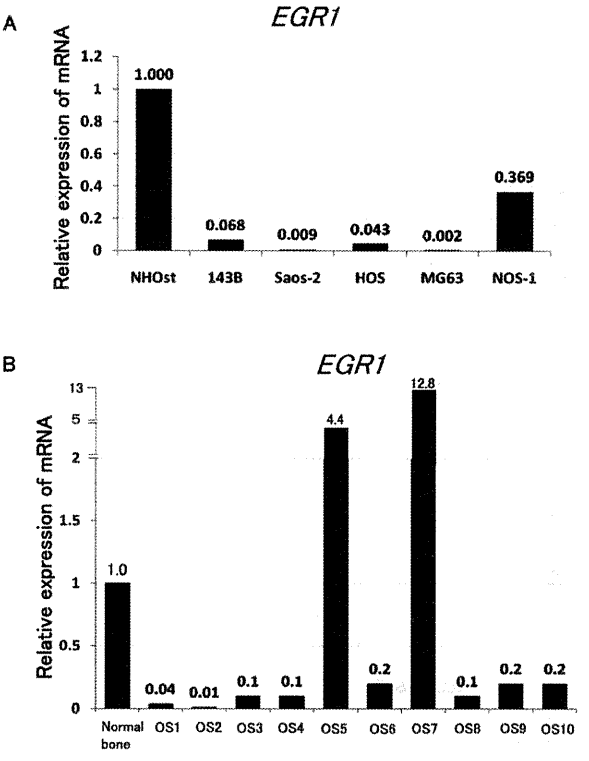

Figure 1. Down-regulation of *EGR1* in human osteosarcoma. Total RNA extracted from osteosarcoma cell lines (A) and osteosarcoma patients' biopsy specimens (B) were analyzed by real-time PCR. Results revealed that 5 of 5 human osteosarcoma cell lines and 8 of 10 human biopsy specimens of osteosarcoma had decreased *EGR1* expression. The comparative Ct (ΔΔCt) method was used to determine fold change in expression using *GAPDH*. These experiments were performed in triplicate with similar results.
doi:10.1371/journal.pone.0016234.g001

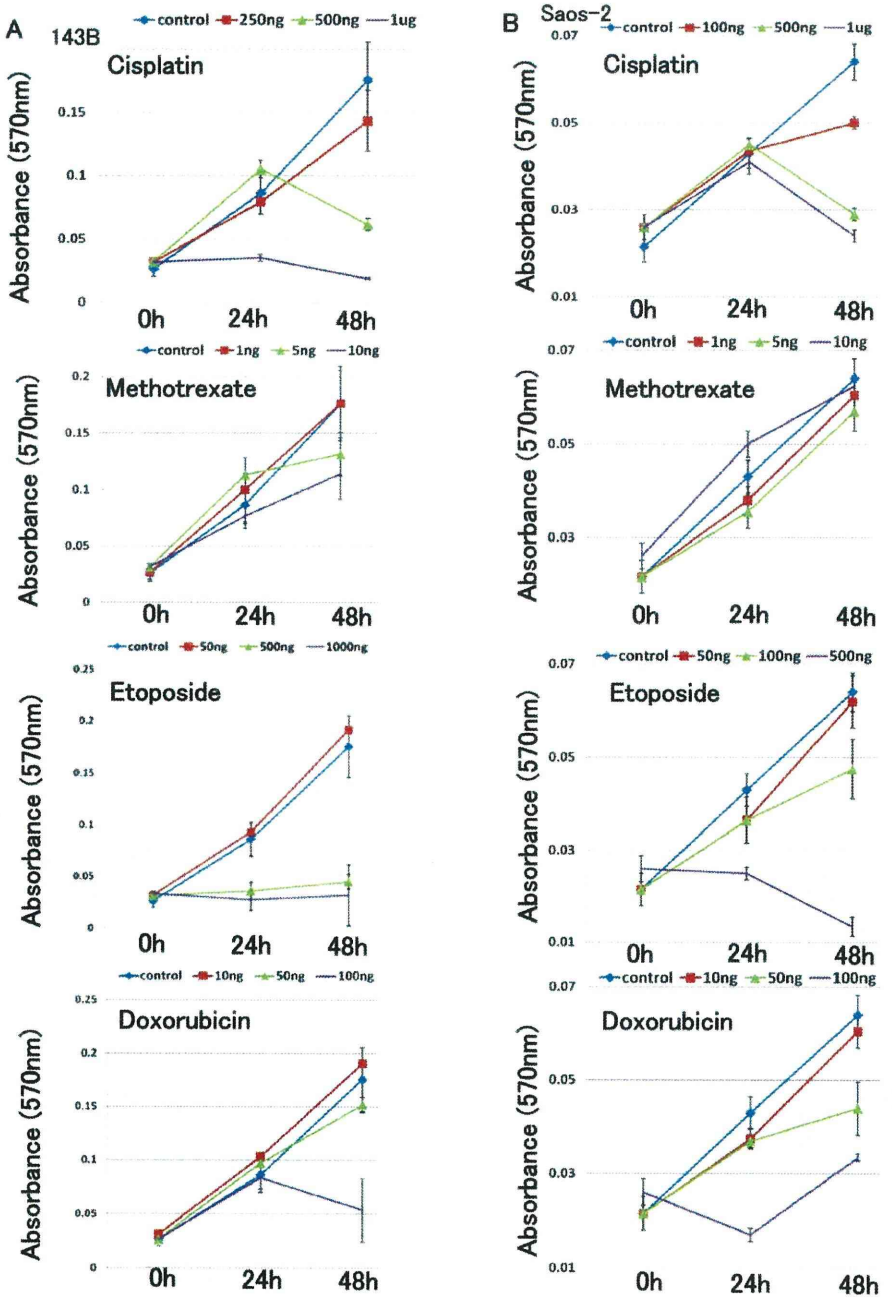

Figure 2. Osteosarcoma cell growth following anti-tumor drug treatment. MTT assay showed that growth at 48 h of 143B cells was not inhibited by 250 ng cisplatin, 1 ng/ml methotrexate, 50 ng/ml etoposide, or 10 ng/ml doxorubicin. Growth of 143B cell was inhibited by higher dose of each drug (*A*) ($P<0.05$). Growth at 48 h of Saos-2 cells was not inhibited by 1 ng/ml methotrexate, 5 ng/ml methotrexate, 10 ng/ml methotrexate, 50 ng/ml etoposide, or 10 ng/ml doxorubicin. Growth of Saos-2 cell was inhibited by higher dose of each drug (*B*) ($P<0.05$). The experiment was performed in triplicate with similar results [error bars represent mean (SD)].
doi:10.1371/journal.pone.0016234.g002

Over-expression of EGR1 does not prevent osteosarcoma growth

It has been reported that EGR1 over-expression suppresses the growth of cell in soft agar and tumor growth in nude mice [10,16]. We therefore, transfected the EGR1 expression vector and examined osteosarcoma cell growth. Western blot analysis showed up-regulation of EGR1 in 143B, Saos-2, and HOS cells (**Figure 4A**). MTT assay revealed that forced expression of EGR1 did not prevent osteosarcoma growth in vitro (**Figure S3A**). We next examined the effects of EGR1 on anchorage-independent osteosarcoma growth. Colony formation assay revealed that forced expression of EGR1 did not affect the

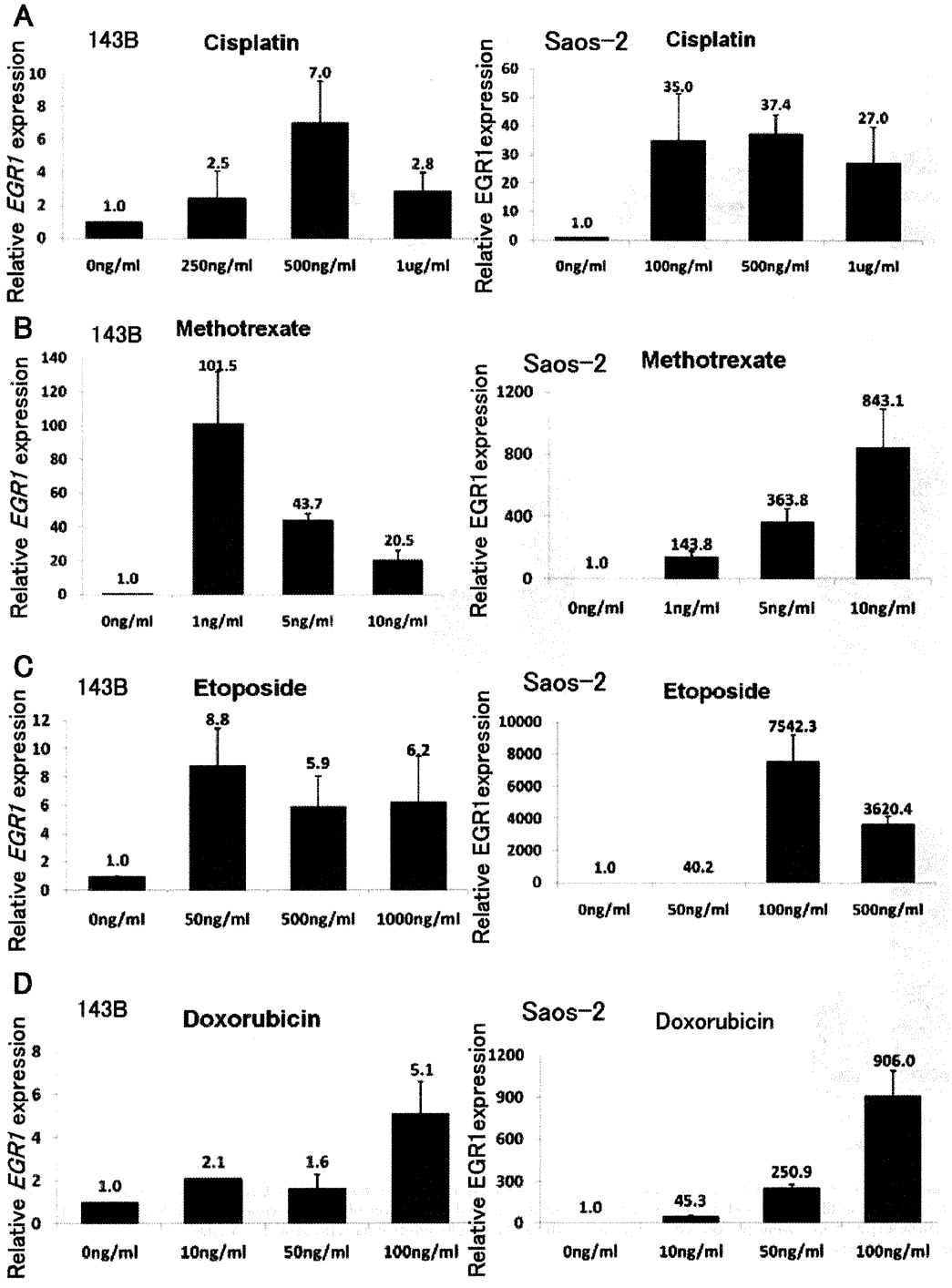

Figure 3. Anti-tumor agent treatment increased the expression of *EGR1*. Following 24 h drug treatments, total RNA extracted from osteosarcoma cell lines were analyzed by real-time PCR. Treatment with cisplatin, methotrexate, etoposide or doxorubicin increased *EGR1* expression in 143B and Saos-2 cells. The comparative Ct (ΔΔCt) method was used to determine fold change in expression using *GAPDH* or *ACTB*. Experiments were performed in triplicate with similar results [error bars represent mean (SD)].
doi:10.1371/journal.pone.0016234.g003

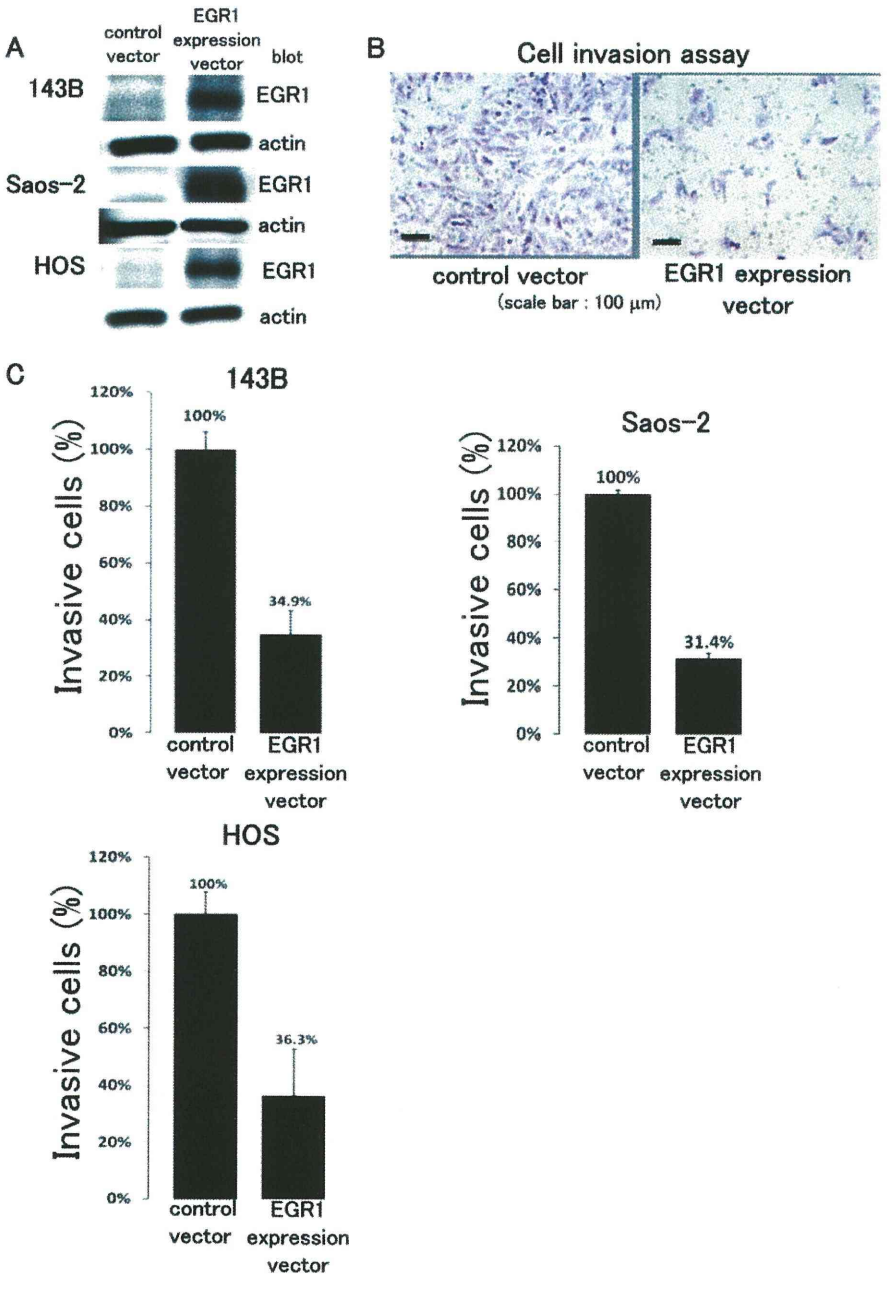

Figure 4. EGR1 prevents osteosarcoma cell invasion in vitro. Western blot analysis revealed that lysates of EGR1 expression vector-transfected cells were positive for anti-EGR1 antibody (*A*). Cell invasion assay showed that forced expression of EGR1 decreased 143B, Saos-2, and HOS cell invasion (*B*) ($P<0.05$). These experiments were performed in triplicate with similar results [error bars represent mean (SD)].
doi:10.1371/journal.pone.0016234.g004

number of colony formation (**Figure S3B**). These findings suggest that up-regulation of EGR1 following anti-tumor agent treatment had no effect on osteosarcoma cell growth.

Over-expression of EGR1 prevents osteosarcoma cell invasion in vitro

To examine the effects of EGR1 up-regulation after anti-tumour agent treatment in modulating the invasive activity of osteosarcoma cells, in vitro invasive activity assays were performed to assess the proportion of osteosarcoma cells transfected with EGR1 expression vector or control vector that invaded through matrigel-coated membranes. Significantly lower proportions of 143B, Saos-2, and HOS cells transiently transfected with EGR1 expression vector migrated through matrigel-coated chambers than osteosarcoma cells transfected with control vector (**Figure 4B, C**).

Down-regulation of uPA and uPAR by EGR1

We then examined the cellular mechanisms by which EGR1 exerts its effects on osteosarcoma cell invasion. Several investigations have shown that EGR1 plays an important role in the control of tumor metastasis through regulation of cancer invasion-related genes, including TGF-β1, thrombospondin-1, and plasminogen activator inhibitor-1 [17,18]. We examined whether EGR1 affects the expression of cancer invasion-related genes. Real-time PCR revealed that forced expression of EGR1 in 143B, Saos-2, and HOS osteosarcoma cell lines decreased the expression of *uPA* and *uPAR* (**Figure 5**). ELISA revealed that forced expression of EGR1 decreased the expression of uPA and uPAR proteins (**Figure S4**). Further, we examine the effects of anti-tumour agents on *uPA and uPAR* expression in vitro, we performed real-time PCR after anti-tumor agent treatment. Treatment of low dose anti-tumor drugs decreased the expression of *uPA* and *uPAR* (**Figure S5**). To examine the effects of low dose chemotherapy on *uPA and uPAR* expression in vivo, we used osteosarcoma murine xenograft model with 143B cells. Nude mice were treated with 4 μg/kg doxorubicin. Real-time PCR showed that low dose doxrubicin

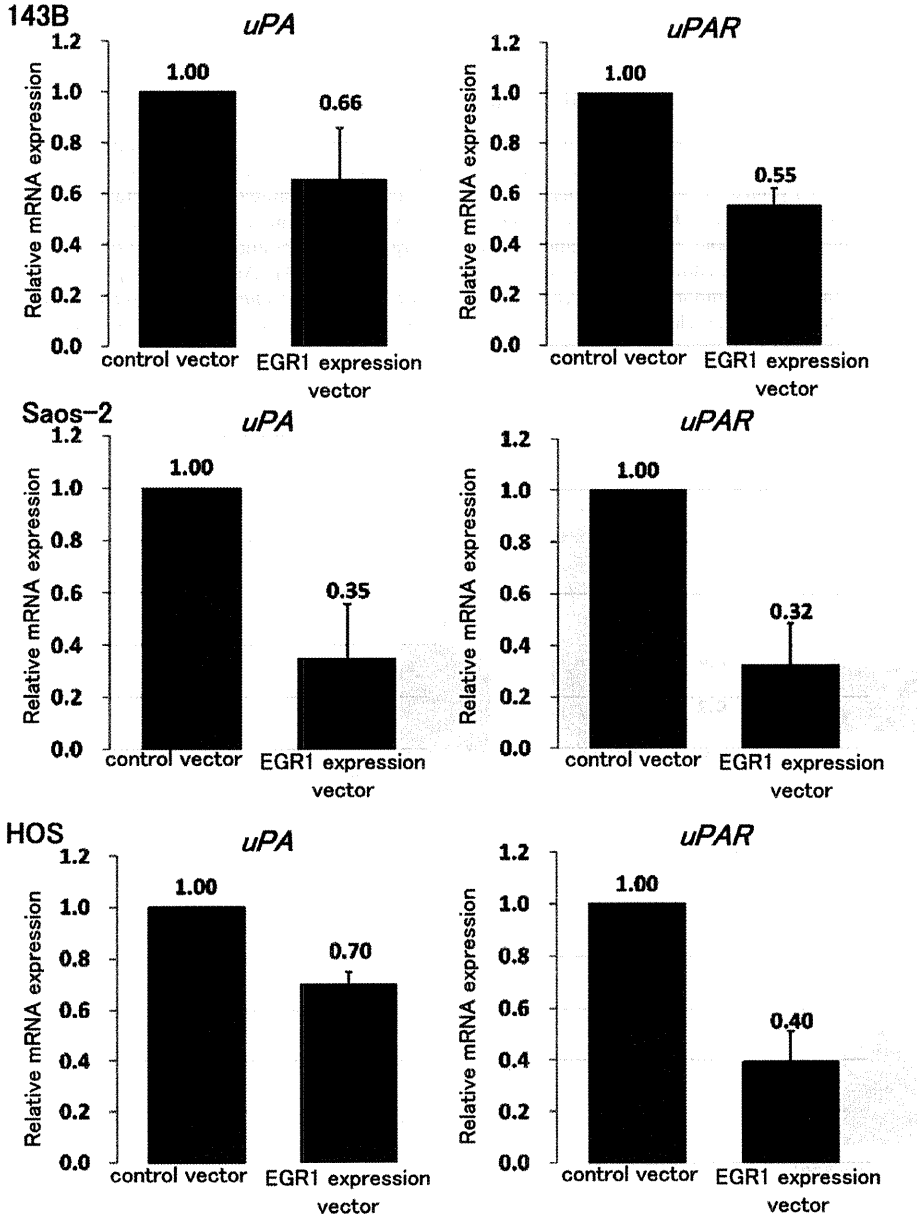

Figure 5. EGR1 decreased expression of *uPA* and *uPAR*. We examined whether EGR1 affects the expression of uPA and uPAR. RNA was prepared from control vector or EGR1 expression vector stably transfected cells. Real-time PCR revealed that forced expression of EGR1 decreased *uPA* and *uPAR* expression in 143B, Saos-2, and HOS cells ($P<0.05$). The comparative Ct (ΔΔCt) method was used to determine fold change in expression using *GAPDH*. These experiments were performed in triplicate with similar results [error bars represent mean (SD)].
doi:10.1371/journal.pone.0016234.g005

treatment decreased expression of *uPA* and *uPAR* in vivo (**Figure S6A**).

EGR1 down-regulates uPA activity

uPA is produced and secreted as an inactive single-chain polypeptide, termed pro-uPA, which lacks plasminogen-activating activity. The binding of pro-uPA to uPAR induces its activation which in turn converts plasminogen to the active serine protease plasmin [19]. In this regard, we examined whether EGR1 exerts effects on uPA activity by performing uPA activity ELISA. ELISA showed that forced expression of EGR1 in osteosarcoma cell lines down-regulated the activity of uPA (**Figure 6**).

EGR1 suppresses osteosarcoma migration into blood vessels in vivo

To investigate the effects of EGR1 on osteosarcoma tumor migration and invasion in vivo, we used a novel osteosarcoma murine xenograft model with 143B cells. Intrajoint inoculation of GFP-positive 143B cells in nude mice induced primary osteosarcoma tumor formation by 2 weeks after inoculation. These primary tumors gave rise to microscopically detectible micro metastases in the lungs within 5 weeks after inoculation. Although we attempted to determine the volume of the primary tumors, we were unable to do so because tumor had extended into muscle and bone. RNA was prepared from tumor formed by control vector or EGR1 expression vector transfected cells. Real-time PCR revealed that forced expression of EGR1 decreased *uPA* and *uPAR* expression in vivo (**Figure S6B**). After 5 weeks, we counted GFP-positive- 143B cells within 50 μl blood aspirates from hearts. The vector control group had an average of 51.2 cells, whereas the EGR1 group averaged only 18.7 cells (**Figure 7A, B**). Lung metastases were found in 6 of 6 control cell-inoculated mice. In contrast, there were lung metastases in 4 of 6 EGR1-expressing 143B-inoculated mice. The percent of lung metastasis area was calculated. The vector control group had an average of 0.6% metastasis area, whereas the EGR1 group averaged 0.31% metastasis area (**Figure 7C**). These findings show that EGR1 prevented osteosarcoma migration into blood vessel in vivo.

Discussion

Current standard regimens for osteosarcoma treatment include preoperative and postoperative chemotherapy. The benefits of chemotherapy have been demonstrated in many studies. Preoperative chemotherapy induces tumor necrosis in the primary tumor facilitating surgical resection and enabling early treatment of micrometastatic disease [20,21]. Among those patients who received neoadjuvant treatment, chemotherapy-related tumor necrosis was good in 62% and poor in 38% of patients [22].

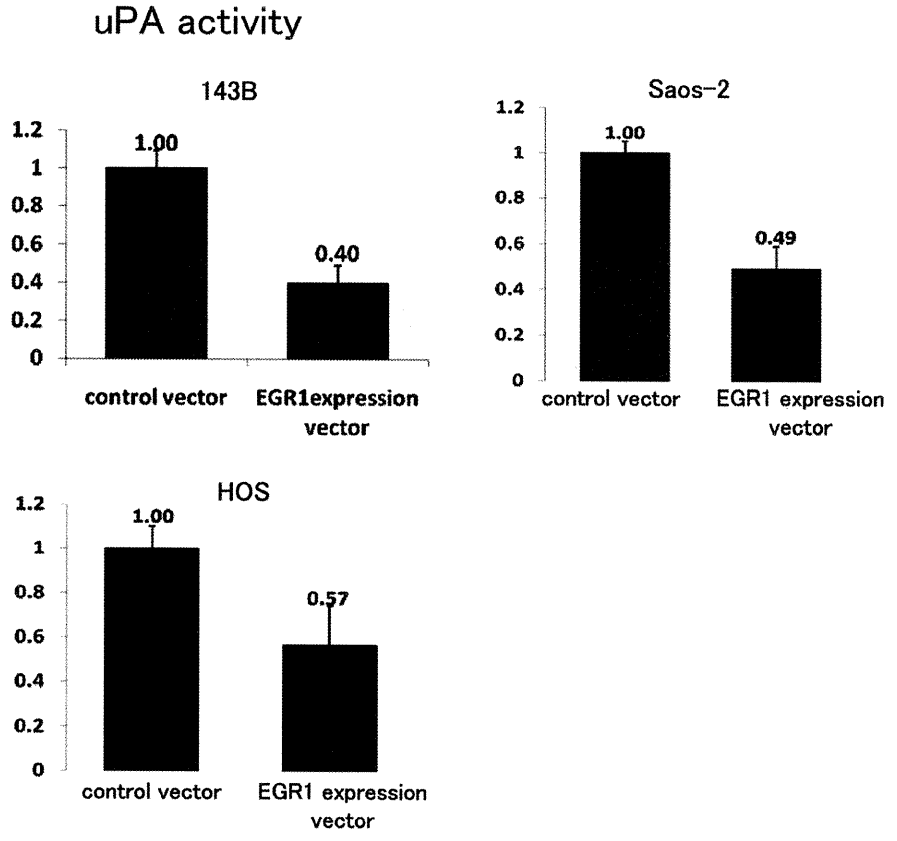

Figure 6. EGR1 decreased uPA activity. uPA activity was examined using cell lysates. Cell lysate were prepared from control vector or EGR1 expression vector transfected cells. ELISA assay showed that EGR1 decreased uPA activity 0.40-fold in 143B (A). uPA activity was decreased 0.49-fold by EGR1 in Saos-2 (B). Luciferase assay showed that EGR1 decreased uPA activity 0.57-fold in HOS (C). These experiments were in triplicate with similar results [error bars represent mean (SD)] ($P<0.05$).
doi:10.1371/journal.pone.0016234.g006